



A TEM study of the incommensurate modulated structure in $\text{Sr}_2\text{CuO}_{3+x}$ superconductors synthesized under high pressure

B. Structural model

H. Zhang ^{a,*}, Y.Y. Wang ^a, L.D. Marks ^a, V.P. Dravid ^a, P.D. Han ^b, D.A. Payne ^b

^a Department of Materials Science and Engineering, Northwestern University, Evanston, IL 60208, USA

^b Department of Materials Science and Engineering, University of Illinois at Urbana-Champaign, Urbana, IL 61801, USA

Received 13 March 1995; revised manuscript received 20 September 1995

Abstract

This paper reports a detailed structural study of the incommensurate modulated phase in high pressure synthesized $\text{Sr}_2\text{CuO}_{3+x}$ superconductors based on transmission electron diffraction, high resolution electron microscopy and simulations. Face-centered orthorhombic structure with an average commensurate lattice constant of about $5\sqrt{2}a_p \times 5\sqrt{2}a_p \times c_p$ (p stands for the tetragonal La_2CuO_4 -type structure) has been identified and an atomic model of this average structure is proposed. The modulated structure results from metal ion shear displacements with half sine and half cosine waves along $\langle 110 \rangle_p$ directions. Analysis of the displacement fields suggests that the Cu ions have a half cosine wave displacement, which supports the existence of oxygen vacancies in the CuO_{1+x} layer proposed by a previous neutron diffraction study. If this modulated phase is indeed the superconducting phase our results call into question the requirement of intact CuO_2 sheets for superconductivity in high- T_c cuprates.

1. Introduction

Part A of this article [1] reported the evolution of the structural and electronic properties as a function of heat treatment in the modulated phases of $\text{Sr}_2\text{CuO}_{3+x}$ superconductors. This superconductor has the interesting features that T_c increases from 70 to 94 K after annealing at 310°C and the volume of the unit cell also slightly increases with this anneal-

ing [2]. The observation that a substantial oxygen K pre-edge exists in the modulated phases of the superconducting samples, but not in the non-superconducting samples, implies that these superstructures might be responsible for superconductivity (see part A [1]). It is therefore important to understand the structural features of these phases; this article will concentrate on a detailed structural study of the modulated phase.

Although the observed modulated structures are actually incommensurate and the modulation wavelength varies slightly with the heat treatments, for simplicity we will model it as an average commensu-

* Corresponding author. Fax: +1-708-491-7820.

rate lattice. The essential structural features are not affected by this treatment. A modulated structure in the $\text{Sr}_2\text{CuO}_{3+x}$ superconductor was first reported by Hiroi et al. [3]. They found that the basic structure is a K_2NiF_4 -type tetragonal cell and the superlattice has a lattice constant of about $4\sqrt{2}a_p \times 4\sqrt{2}a_p \times c_p$, where p stands for the primary K_2NiF_4 -type structure. By iodometric titration the oxygen content was estimated to be 3.1. Assuming the existence of intact CuO_2 sheets which is believed to be a requirement for superconductivity in the high- T_c cuprates, both Hiroi et al. [3] and Adachi et al. [4] proposed a model in which almost half the oxygen atoms are missing in the ideal Sr_2O_2 layers. They assumed that the superlattice was formed by the ordering of these oxygen vacancies. Later, Laffez et al. [5] reported a different superstructure with a lattice constant of

$5\sqrt{2}/2a_p \times 5\sqrt{2}/2a_p \times c_p$ but did not present a detailed study of the structure. Recently Shimakawa et al. [6] studied $\text{Sr}_2\text{CuO}_{3+x}$ using neutron diffraction and reported that the basic structure is an oxygen-deficient La_2CuO_4 -type tetragonal T structure with oxygen vacancies located in the CuO_2 layers instead of in the Sr_2O_2 layers. A simplified structural model of atomic displacements with sinusoidal waves along two perpendicular $[110]_p$ type directions was proposed to explain the $4\sqrt{2}a_p \times 4\sqrt{2}a_p \times c_p$ superstructure and the amplitudes of the modulated waves were refined.

Based on transmission electron diffraction patterns (EDPs), high resolution electron microscopy (HREM) images, and simulations, we are able to determine a detailed cation structure of the modulated compound in our samples and consequently

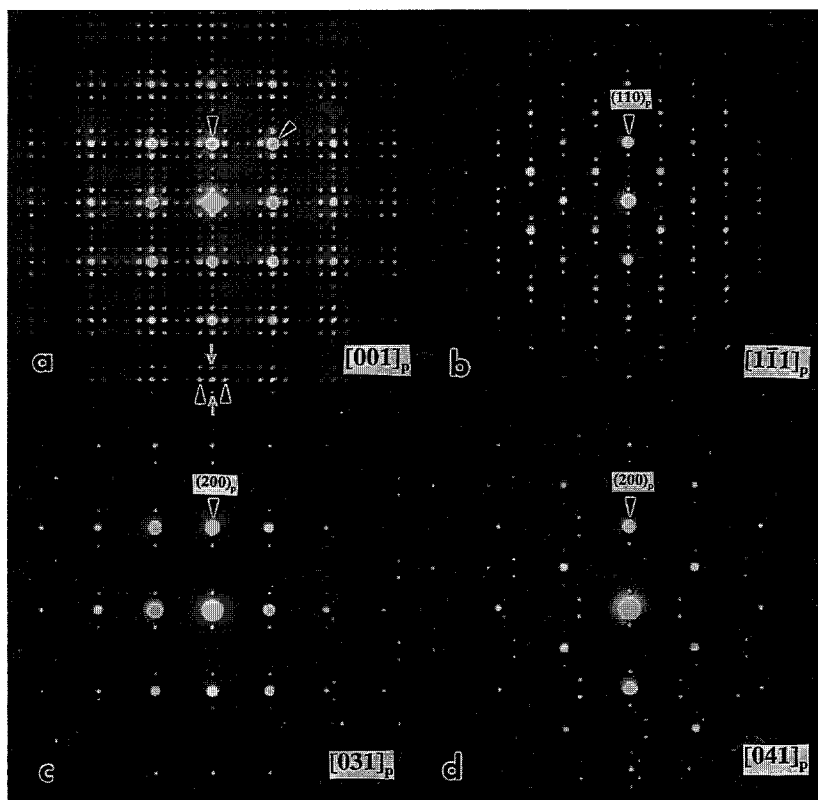


Fig. 1. A set of diffraction patterns of the modulated structure in 70 K T_c as-grown $\text{Sr}_2\text{CuO}_{3+x}$ superconductors showing a face-centered $5\sqrt{2}a_p \times 5\sqrt{2}a_p \times c_p$ orthorhombic superstructure.

derive the probable positions of the oxygen atoms from the cation structure.

2. Experimental

The low-pressure form of Sr_2CuO_3 was synthesized by mixing high-purity SrCO_3 , CaCO_3 and CuO fine powders and reacting these powders at 935°C in dry air and subsequently at 1150°C in a 160 bar pure oxygen atmosphere. The powder was then pressed into pellets, sandwiched between two thin KClO_4 pellets, sealed in a gold capsule and then subjected to a high pressure and high temperature anneal. KClO_4 which releases oxygen upon decomposition at high temperature acted as an internal oxidizer for the oxide powder. The synthesis conditions were 4–6

GPa pressure and between 800 – 1150°C for 30–60 min. The as-prepared samples have an onset T_c of 70 K with a 15% Meissner fraction which indicates bulk superconductivity. A T_c of 94 K was achieved by annealing in N_2 at 310°C for 30 min, and superconductivity vanished upon annealing at 450°C . More details about the sample synthesis and the properties are reported by Han et al. [2].

TEM thin foils were prepared by conventional techniques, i.e. mechanical thinning followed by dimpling and ion milling. A liquid nitrogen cold stage was used for ion milling to reduce ion beam damage. HREM images and EDPs were obtained on a Hitachi H9000 microscope operated at 300 kV and a Hitachi Field-emission gun HF2000 microscope operated at 200 kV. Large angle tilt diffraction was performed on a Philips CM30 operated at 300 kV.

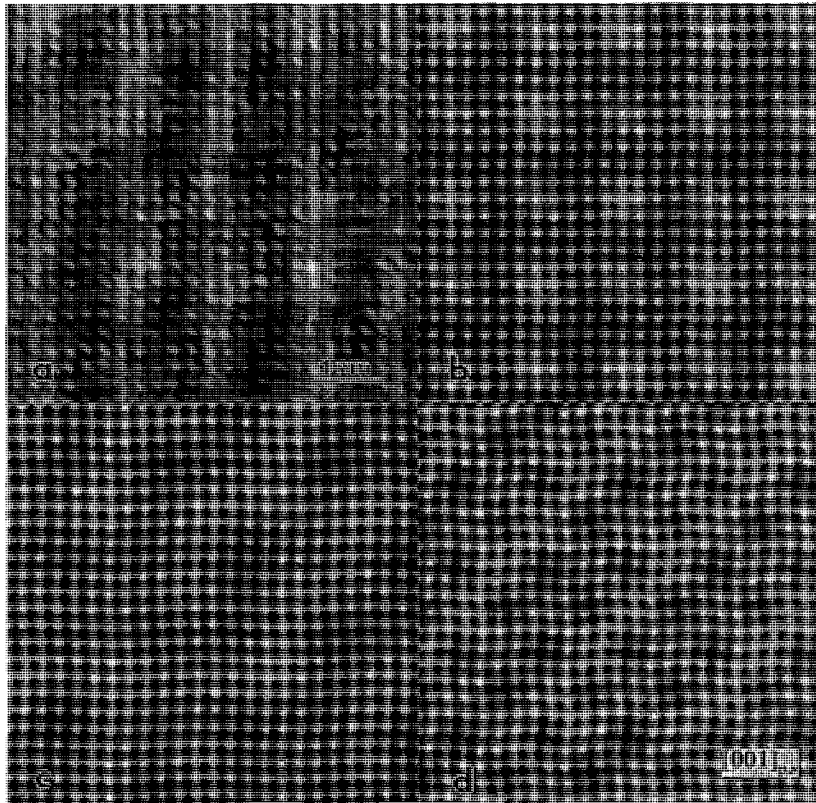


Fig. 2. Experimental and simulated HREM images from different models along the $[001]_p$ direction. (a) experimental image, (b) simulated image with the correct model (see text), (c) simulated image with sinusoidal waves along $[110]_p$ directions with a periodicity of $5\sqrt{2}a_p$, (d) simulated image with a model similar to (c) but with half the periodicity for the modulated waves.

HREM image and electron diffraction simulations were carried out using NUMIS multislice programs on Apollo workstations.

3. Results and discussion

3.1. Electron diffraction

Fig. 1 shows a set of diffraction patterns tilted from the $[001]_p$ zone axis along both $g_{(200)_p}$ and $g_{(110)_p}$ reciprocal directions of the $\text{Sr}_2\text{CuO}_{3+x}$ modulated structure in the as-grown samples with a T_c of 70 K. All the basic strong reflections can be indexed using a body-centered La_2CuO_4 lattice with $I4/mmm$ space group and lattice constants of about $a_p = 3.76$ and $c_p = 12.55$ Å as reported by Shimakawa et al. [6]. In Fig. 1(a) the superstructure spots form a two-dimensional lattice with a unit cell about 5 times the $(110)_p$ spacing along both $[110]_p$ and $[1\bar{1}0]_p$ directions. However, the patterns in Figs. 1(b) and 1(d) show centered rectangular unit cells giving doubling of the lattice constants along these two directions. Furthermore, the EDP along the $[010]_p$ direction in Fig. 4(b) (shown later) does not indicate any modulation along the c_p axis. Thus the lattice constants of the superstructure are about $5\sqrt{2}a_p \times 5\sqrt{2}a_p \times c_p$. Based on this supercell the (hkl) reflection conditions were all odd or all even, which indicates that the superstructure is face-centered. Then for the $[001]_p$ diffraction pattern both h and k are even in the supercell. We note an important feature of Fig. 1(a) namely that the superstructure spots (black arrows) along the directions perpendicular to the modulation directions $[110]_p$ and $[1\bar{1}0]_p$ (or $[100]_s$ and $[010]_s$, s denotes the superstructure) are stronger than those along directions parallel to them (marked by the white arrows). We will see that this reflects an essential feature of the structure.

3.2. Shear displacements of the metal ions and the structural model

As shown by the HREM images in Fig. 2(a) taken along the $[001]_{p,s}$ direction, the modulation is quite strong in images from the thin regions. This means that the strongly scattering metal cations are perturbed. Since there are only two metal elements in

this compound and the stoichiometry is consistent with a La_2CuO_4 type structure, we assume that only displacements with no chemical modulations exist.

If the original crystal potential $V_0(\mathbf{r})$ of the compound is expressed as:

$$V_0(\mathbf{r}) = \sum V_g \exp(2\pi i \mathbf{g} \cdot \mathbf{r}), \quad (1)$$

where \mathbf{g} is the vector of the original structure in reciprocal space and V_g the amplitude along the specific vector \mathbf{g} , the potential after displacement is:

$$V(\mathbf{r}) = \sum V_g \exp[2\pi i \mathbf{g} \cdot (\mathbf{r} + \mathbf{R})], \quad (2)$$

with $\mathbf{R}(\mathbf{r})$ the displacement field. Assuming that \mathbf{R} is small, this can be expanded as a Taylor series:

$$V(\mathbf{r}) = \sum (2\pi i \mathbf{g} \cdot \mathbf{R} + 1) V_g \exp(2\pi i \mathbf{g} \cdot \mathbf{r}), \quad (3)$$

ignoring the second and higher order terms in \mathbf{R} . Expand $\mathbf{R}(\mathbf{r})$ as:

$$\mathbf{R}(\mathbf{r}) = \sum \mathbf{d}_q \exp(2\pi i \mathbf{q} \cdot \mathbf{r}),$$

where \mathbf{q} is a wave vector and \mathbf{d}_q the displacement vector associated with the wave \mathbf{q} , then:

$$V(\mathbf{r}) = \sum V_g \exp(2\pi i \mathbf{g} \cdot \mathbf{r}) + \sum V_g (2\pi i \mathbf{g} \cdot \mathbf{d}_q) \exp[2\pi i (\mathbf{g} + \mathbf{q}) \cdot \mathbf{r}]. \quad (4)$$

The first term of the expression (4) is the potential of the basic structure, the second the potential of the superstructure at $\mathbf{g} + \mathbf{q}$ in reciprocal space. From the $[001]$ diffraction pattern in Fig. 1a, the spots are strong when \mathbf{g} is perpendicular to \mathbf{q} along both $[110]_p$ and $[1\bar{1}0]_p$ directions. From (4), \mathbf{d}_q is primarily perpendicular to the \mathbf{q} . $\mathbf{R}(\mathbf{r})$ can then be written as:

$$\mathbf{R}(\mathbf{r}) = \sum \{ x \alpha q \exp(2\pi i q y) + y \beta q \exp(2\pi i q x) \}.$$

The HREM image in Fig. 2(a) confirms this displacement field and implies a simple sine- or cosine-like displacement.

The above result agrees with the model proposed by Shimakawa et al. [6] who assumed a sinusoidal atomic displacement wave $x = x + \alpha_* \sin(2\pi y)$, $y = y + \alpha_* \sin(2\pi x)$. This model with an amplitude of about 0.23 Å for all the atoms and a wavelength about 10 times $[110]_p$ along two perpendicular $[110]_p$

and $[1\bar{1}0]_p$ directions was simulated. The amplitude used here is obtained from neutron data refined on the $4\sqrt{2}a_p \times 4\sqrt{2}a_p \times c_p$ structure, and for simplification the same value was used for all atoms, although slightly different values were refined for different atoms [6]. In the following simulation we assume that half the oxygen atoms are missing in the CuO_2 planes and the remaining oxygen atoms are randomly distributed in the plane. In the later discussion we will see that the oxygen atoms are actually not randomly distributed in each Cu–O plane, but this assumption does not affect the results.

The simulated image along $[001]$ is shown in Fig. 2(c). The thickness and defocus for the simulation are about 50 and -500 \AA respectively. The image shows island-like dark and white contrast similar to the experimental HREM image in Fig. 2(a), however, the dark contrast varies along a direction which is 45° from the modulation directions instead of parallel to them. Furthermore, the periodicity of the superstructure is not correct. The image shown in Fig. 2(d) calculated using the same model but with half the periodicity gives the right periodicity, however the contrast is still not correct. Detailed analysis of the displacement fields showed that the half cosine wave in Fig. 2(c) along both directions matched the experimental contrast. (A half cosine wave is here a half part of a full cosine wave, i.e. the wave from 0 to π , similarly for a half sine wave.) Fig. 3 illustrates these waves in one dimension. A discontinuity at the boundaries of the half cosine waves is apparent as shown in Fig. 3(b). We will see later that this is actually an essential structural feature. Combined with the diffraction results, we propose a structural model where the CuO_{1+x} layers have a half cosine wave displacement field and the Sr_2O_2 layers a half sine wave displacement field with a periodicity of $5\sqrt{2}a_p$. Fig. 2(b) is the simulated image. The reason why CuO_{1+x} has a half cosine wave displacement field will be discussed later. Images calculated based on models of the displacements with only half cosine or half sine waves for all the atoms do not match the experimental images.

Figs. 4(a) and 4(c) show two members of a through-focal series of experimental HREM images. The corresponding simulated images based on our proposed model are shown in Figs. 4(b) and 4(d). Fairly good agreement is evident. In the simulated

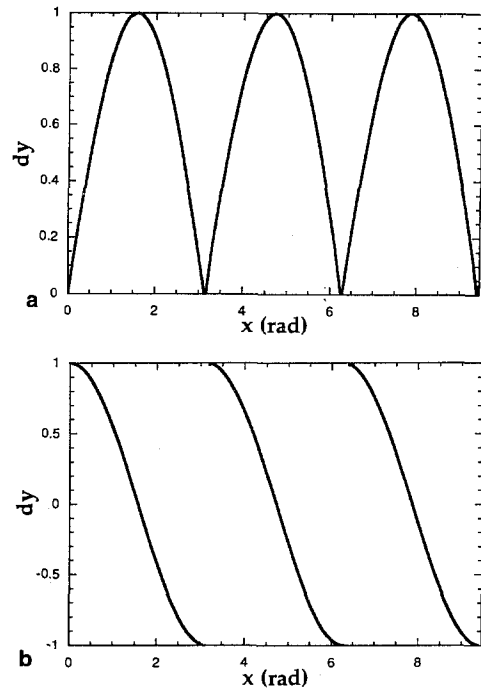


Fig. 3. One-dimensional illustration of half sine and half cosine waves: (a) the half sine wave, (b) the half cosine wave showing a discontinuity at the boundaries.

image shown in Fig. 4(d), “atoms” are closer together in the white regions, which is consistent with the experimental image in Fig. 4(c). The thickness for the simulations is about 75 \AA and the defoci are -550 and -1080 \AA for Fig. 4(b) and Fig. 4(d) respectively. The defoci were calibrated by comparing the power spectra of the amorphous edge of the experimental images with simulated contrast transfer functions. They also match the value predicted by the nominal 10 nm focal step. Other through-focal experimental images (not shown here) also agree with the simulated images. Fig. 5 shows a montage of experimental EDPs viewed along $[001]_{p,s}$ and $[010]_p$ (or $[110]_s$) and the corresponding simulated diffraction patterns; a fairly good agreement is seen in both cases. The weak spot, indicated by an arrow in the simulated EDP of Fig. 5(c) is from the higher order Laue zone. The above analysis is only semi-quantitative and a more quantitative study would be useful, but exceedingly difficult for a large cell incommensurate structure.

As we pointed out before, the half cosine wave displacement fields result in a discontinuity at the boundaries. From a structural point of view this discontinuity must be associated with a defect. In the low pressure form only CuO chain layers exist and since the neutron diffraction study [6] revealed oxygen vacancies in the CuO₂ layers in the high pressure form, it is reasonable to assume that the half cosine wave displacement modulation is in the CuO_{1+x} layers and that the defects are oxygen vacancies.

Fig. 6(a) shows the configuration of Cu ions projected along the [001]_{p,s} direction with a half cosine wave displacement field. The filled and open circles represent the different Cu ions in the two different CuO_{1+x} planes along the *c* axis. A $5\sqrt{2}a_p$

$\times 5\sqrt{2}a_p$ large unit cell is illustrated in the picture and is a centered orthorhombic structure. Fig. 6(b) shows a projection of the modulated and unmodulated Cu positions along the *c* axis. The filled circles denote the modulated Cu ion positions and the open circles the unmodulated Cu ion positions. At the boundaries between the half cosine waves there are shear displacements (arrowed) which give rise to stacking fault-like defects. Between the boundaries the Cu ions are compressed along the [100]_p direction and dilated along [010]_p (arrowed). In contrast, at the boundaries, the spacing along [100]_p is larger than that along [010]_p due to the shear displacements and the long Cu–Cu spacing is about $4.02 \pm 0.02 \text{ \AA}$ (except for an odd point at the corner), the short Cu–Cu spacing about $3.56 \pm 0.02 \text{ \AA}$ (except for an

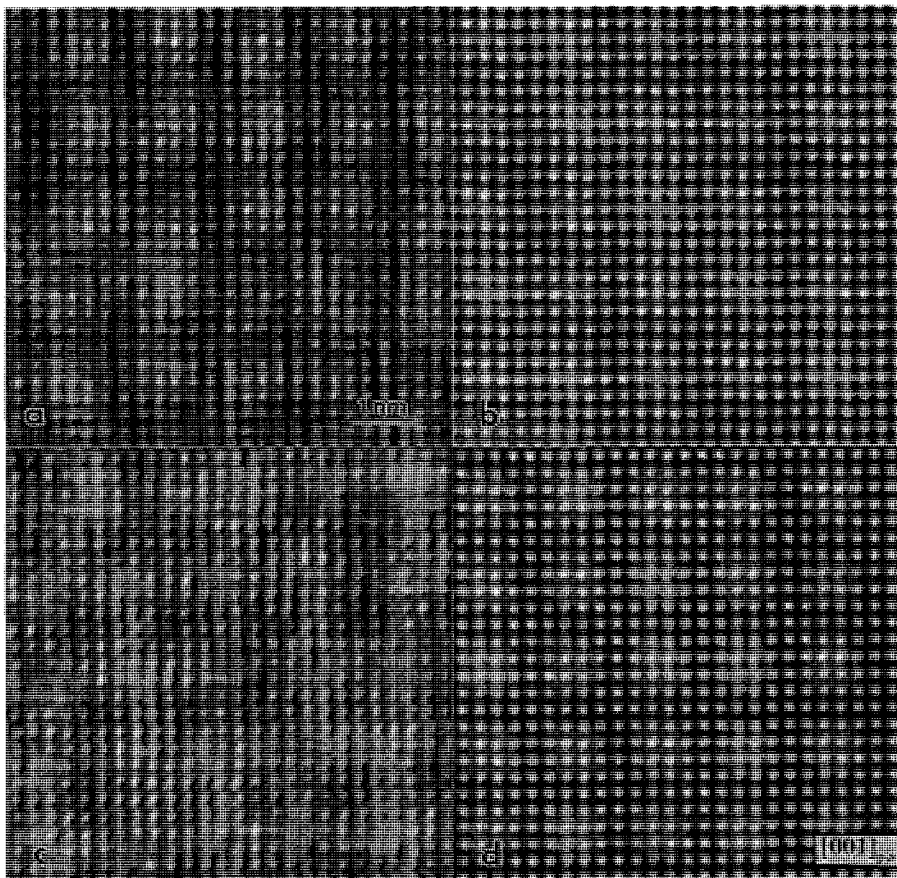


Fig. 4. Two members (a) and (c) from a set of through-focal experimental HREM images and corresponding simulated images (b) and (d) along the [001]_p direction. Defoci for the simulated images (b) and (d) are -55 nm and -108 nm respectively, and the thickness is 7.5 nm .

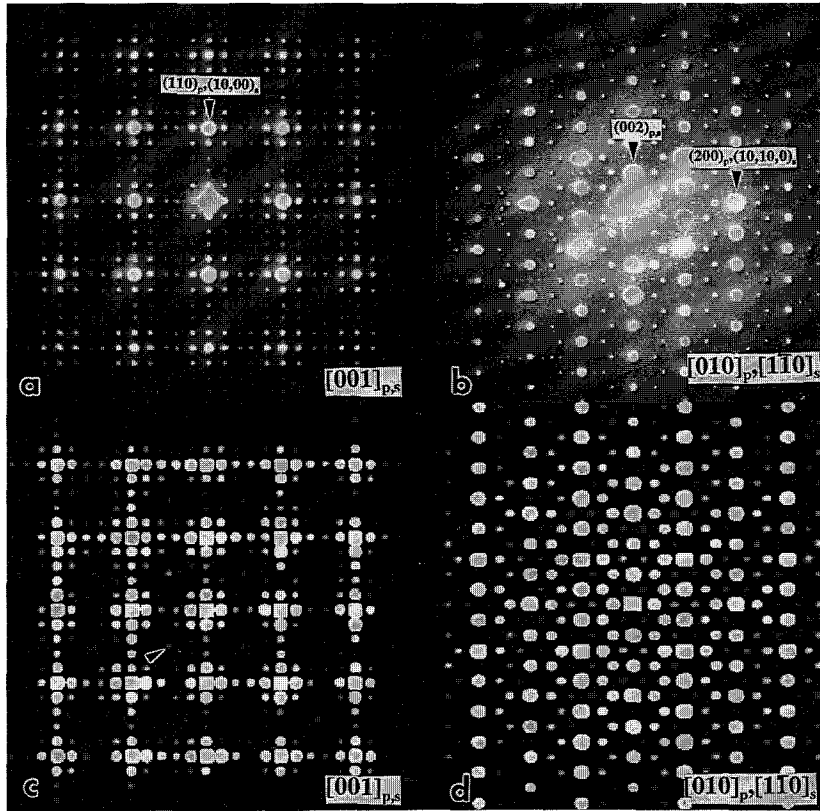


Fig. 5. Experimental and corresponding simulated EDPs of the modulated structure along the $[001]_{p,s}$ (a) and (c), $[010]_p$ or $[110]_s$ (b) and (d) directions.

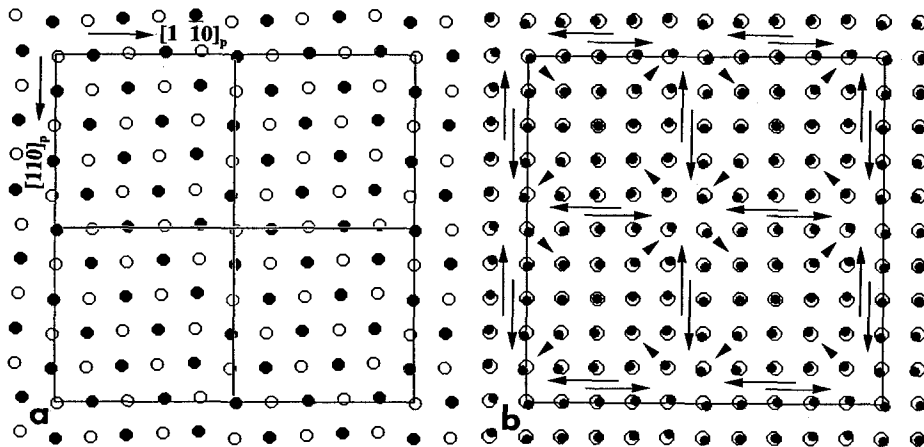


Fig. 6. (a) Configuration of the Cu ions projected along the c axis with a half cosine wave displacement. Filled and open circles represent the two different Cu ions in two different layers along the c axis. The unit cell is represented by lines and has a centered structure. (b) The superposed projection of the modulated Cu ion positions (filled circles) and the unmodulated Cu ion positions (open circles) show the displacement field.

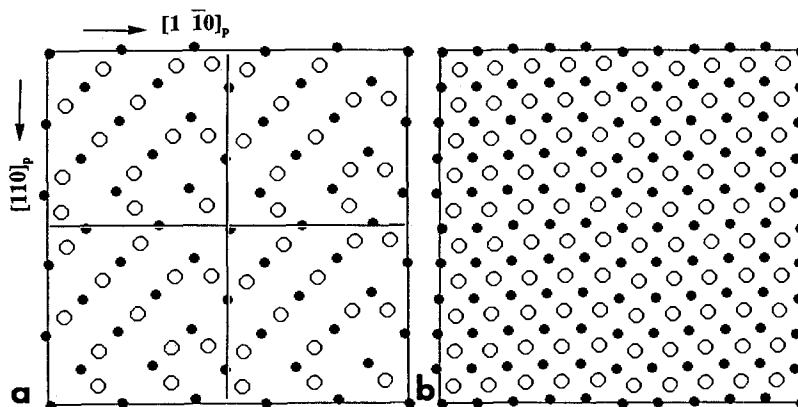


Fig. 7. (a) A possible atomic configuration of one CuO layer along the c axis outlined (assuming that half the oxygen atoms are missing). Filled circles denote Cu ions and open circles O ions. (b) projection of two CuO layers along the c axis.

odd point at the corner). Between the boundaries, the long Cu–Cu spacing is about $3.93 \pm 0.04 \text{ \AA}$ (relatively short compared to the value at the boundaries), and the short Cu–Cu spacing $3.62 \pm 0.04 \text{ \AA}$ (relatively long). If we assume that oxygen ions exist only between dilated Cu ions and that no oxygen ions exist between compressed Cu ions, then half the oxygen atoms would be missing in this plane.

Fig. 7(a) outlines the configuration of the Cu–O layer with half the oxygen atoms missing based on the above discussion. The filled circles denote the Cu ions and the open circles O ions. It is obvious that no

CuO₂ square planes exist only Cu–O–Cu chains. The Cu–O–Cu chain is along the $[100]_p$ direction at the boundaries but along the $[010]_p$ direction between the boundaries. The two Cu–O layers have the same configuration, but shifted by a vector of $1/2[111]_p$. Then the two projected Cu–O layers along $[001]_{p,s}$ give oxygen atoms in all possible sites but with 50% occupancy as shown in Fig. 7(b). There are a few points we would like to clarify. First, the Cu–Cu spacing is calculated based on the amplitude value (0.23 \AA) refined by the neutron diffraction for $4\sqrt{2}a_p \times 4\sqrt{2}a_p \times c_p$ [6] and it is only

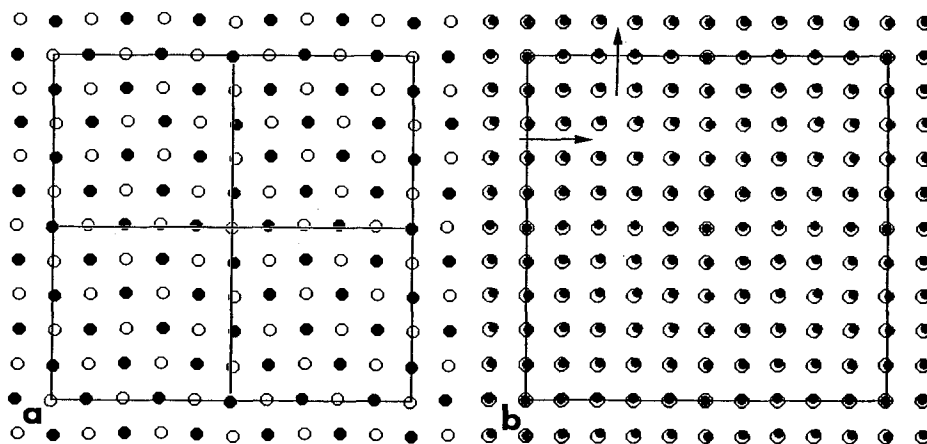


Fig. 8. Similar to Fig. 6, (a) configuration of the Sr ions of the superstructure projected along the $[001]_p$ direction with a sinusoidal displacement wave. (b) shows the displacement field of the Sr ions.

applied to the average commensurate structure; second, there is no direct experimental evidence for the oxygen atom positions.

Fig. 8 shows the atomic configuration and the displacement field of the Sr ions projected along the $[001]_{p,s}$ directions. A centered structure is formed and the displacement field is relatively simple. The directions of the shear are marked by arrows, and the distance between the Sr ions overall is not significantly changed.

From the above discussion the displacement field of the Cu ions is complicated and consistent with substantial depletion of oxygen in the CuO_{1+x} plane. It is reasonable that this structure is metastable due to the inhomogeneous strain field in Fig. 6 and Fig. 8. We speculate that the incommensurate structure (discussed in part A) results from a slight adjustment of the metal ion positions by incorporation of oxygen atoms which provide the charge carriers. Therefore, the structure can change with treatment, here specifically changes of the modulation wavelength (see part A). If the modulated phase is indeed superconducting then this atomic configuration of CuO_{1+x} layers would be very important in understanding the nature of the superconductivity because it is believed that intact CuO_2 square planes are necessary for superconductivity in high- T_c cuprates.

Acknowledgements

The research was supported by the National Science Foundation (DMR 91-20000) through the Science and Technology Center for Superconductivity. We acknowledge the use of the facilities in the Electron Microscope Center at Argonne National Laboratory and also are grateful for stimulating discussions with J.D. Jorgensen at Argonne.

References

- [1] Y.Y. Wang, H. Zhang, V.P. Dravid, L.D. Marks, P.D. Han and D.A. Payne, *Physica C* 255 (1995) 247.
- [2] P.D. Han, L. Chang and D.A. Payne, *Physica C* 228 (1994) 129.
- [3] Z. Hiroi, M. Takano, M. Azuma and Y. Takeda, *Nature (London)* 364 (1993) 315.
- [4] S. Adachi, H. Yamauchi, S. Tanaka and N. Mori, *Physica C* 212 (1993) 164.
- [5] P. Laffez, X.J. Wu, S. Adachi, H. Yamauchi and N. Mori, *Physica C* 222 (1994) 303.
- [6] Y. Shimakawa, J.D. Jorgensen, J.F. Mitchell, B.A. Hunter, H. Shaked, D.G. Hinks, R.L. Hitterman, Z. Hiroi and M. Takano, *Physica C* 228 (1994) 73.